

Supporting Information

Circularly polarized luminescence in one-dimensional assembly of Binaphthyl-based Yb(III) single-molecule magnets

Carlo Andrea Mattei,¹ Vincent Montigaud,¹ Bertrand Lefeuvre,¹ Vincent Dorcet,¹ Gilles Argouarch,¹ Olivier Cador,¹ Boris Le Guennic,¹ Olivier Maury,² Claudia Lalli,¹ Yannick Guyot,³ Stéphan Guy,³ Cyprien Gindre,^c Amina Bensalah-Ledoux,³ François Riobé,^{*2,4} Bruno Baguenard,^{*3} Fabrice Pointillart^{*1}

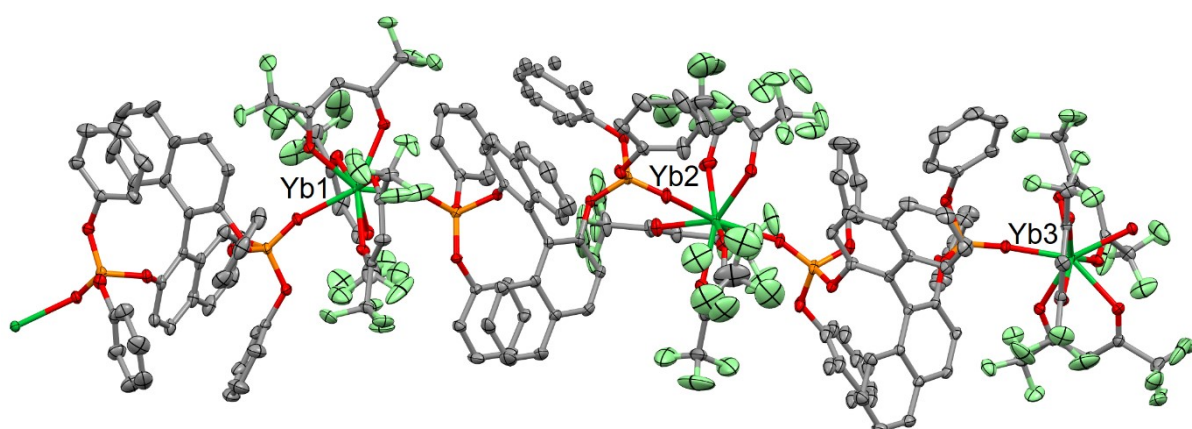


Figure S1. Ortep View of $[(S)-1]_n$. Thermal ellipsoids are drawn at 30% probability. Hydrogen atoms are omitted for clarity.

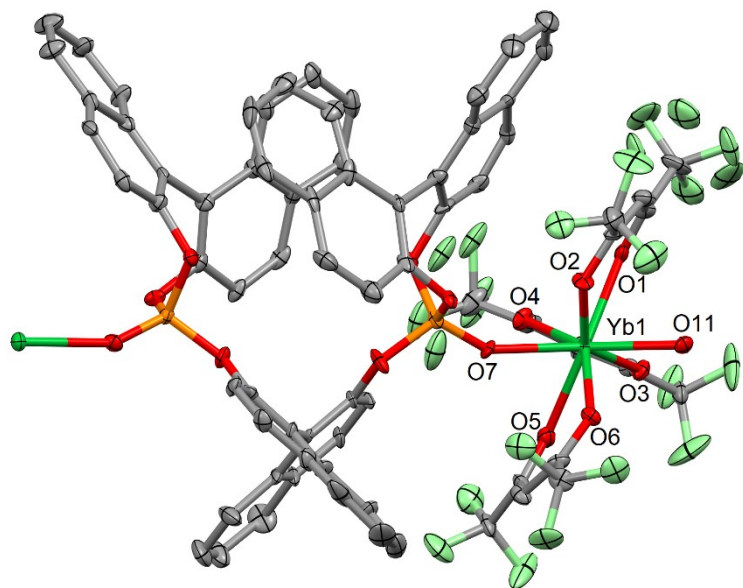


Figure S2. Ortep View of $[(S,S,S)-2]_n$. Thermal ellipsoids are drawn at 30% probability. Hydrogen atoms are omitted for clarity.

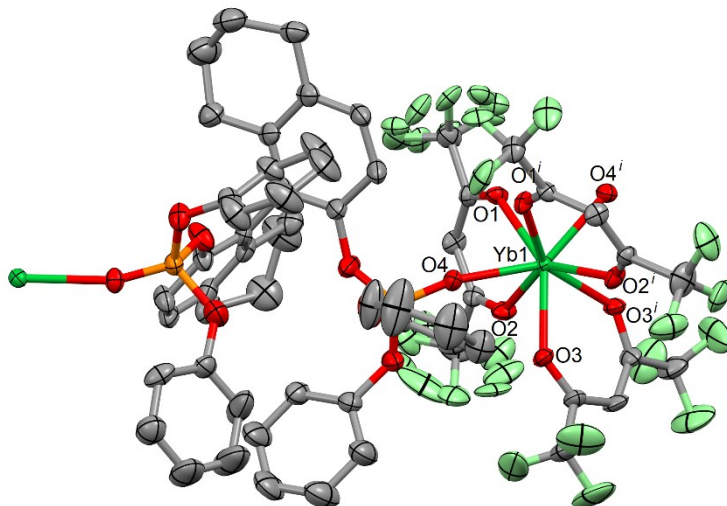


Figure S3. Ortep View of $[(S)-3]_n$. Thermal ellipsoids are drawn at 30% probability. Hydrogen atoms are omitted for clarity.

Table S1. X-ray crystallographic data for $[(S)-1]_n$, $[(S,S,S)-2]_n$ and $[(S)-3]_n$.

Compound	$\{[\text{Yb}(\text{hfac})_3(\text{S-L}^1)]_3\}_n$ $[(S)-1]_n$	$\{[\text{Yb}(\text{hfac})_3(\text{S,S,S-L}^2)]\}_n$ $[(S,S,S)-2]_n$	$\{[\text{Yb}(\text{hfac})_3(\text{S-L}^3)]\}_n$ $[(S)-3]_n$
Formula M / g.mol ⁻¹	C ₁₇₇ H ₁₀₅ Yb ₃ F ₅₄ O ₄₂ P ₆ 4634.54	C ₇₅ H ₃₉ YbF ₁₈ O ₁₄ P ₂ 1741.04	C ₅₉ H ₄₃ YbF ₁₈ O ₁₄ P ₂ 1552.91
Crystal system	Monoclinic	Orthorhombic	Trigonal
Space group	P2 ₁ (N°4)	P2 ₁ 2 ₁ 2 ₁ (N°19)	P3112 (N°151)
Cell parameters	a = 12.037(4) Å b = 35.712(10) Å c = 21.483(6) Å β = 90.942(6)°	a = 16.0519(16) Å b = 21.823(2) Å c = 25.285(3) Å	a = 13.081(2) Å b = 13.081 Å c = 32.167(5) Å γ = 120°
Volume / Å ³	9234(5)	8857.5(17)	4766.7(17)
Z	4	4	3
T / K	150(2)	150(2)	150(2)
2θ range /°	4.08 ≤ 2θ ≤ 55.14	5.83 ≤ 2θ ≤ 54.97	4.40 ≤ 2θ ≤ 55.02
ρ _{calc} / g.cm ⁻³	1.667	1.306	1.623
μ / mm ⁻¹	1.690	1.183	1.637
Number of reflections	254647	46423	38523
Independent reflections	42252	18261	7273
R _{int}	0.0296	0.1198	0.0689
Fo ² > 2σ(Fo) ²	40473	12626	6157
Number of variables	2718	1011	293
Flack parameter	0.013(3)	-0.017(8)	0.026(17)
R ₁ , ωR ₂	0.0228, 0.0544	0.0951, 0.2759	0.0514, 0.1005

Table S2. Cell parameters for $[(S,S,S)-4]_n$

Compound	$\{[\text{Yb}(\text{hfac})_3((\text{S,S,S}-\text{L}^4)]\}_n$ $[(S,S,S)-4]_n$
Formula M / g.mol ⁻¹	C ₇₅ H ₆₃ YbF ₁₈ O ₁₄ P ₂ 1764
Crystal system	Orthorhombic
Cell parameters	a = 19.4340(18) Å b = 19.4340 Å c = 26.6722(24) Å
Volume / Å ³	10073.6(18)
T / K	150(2)

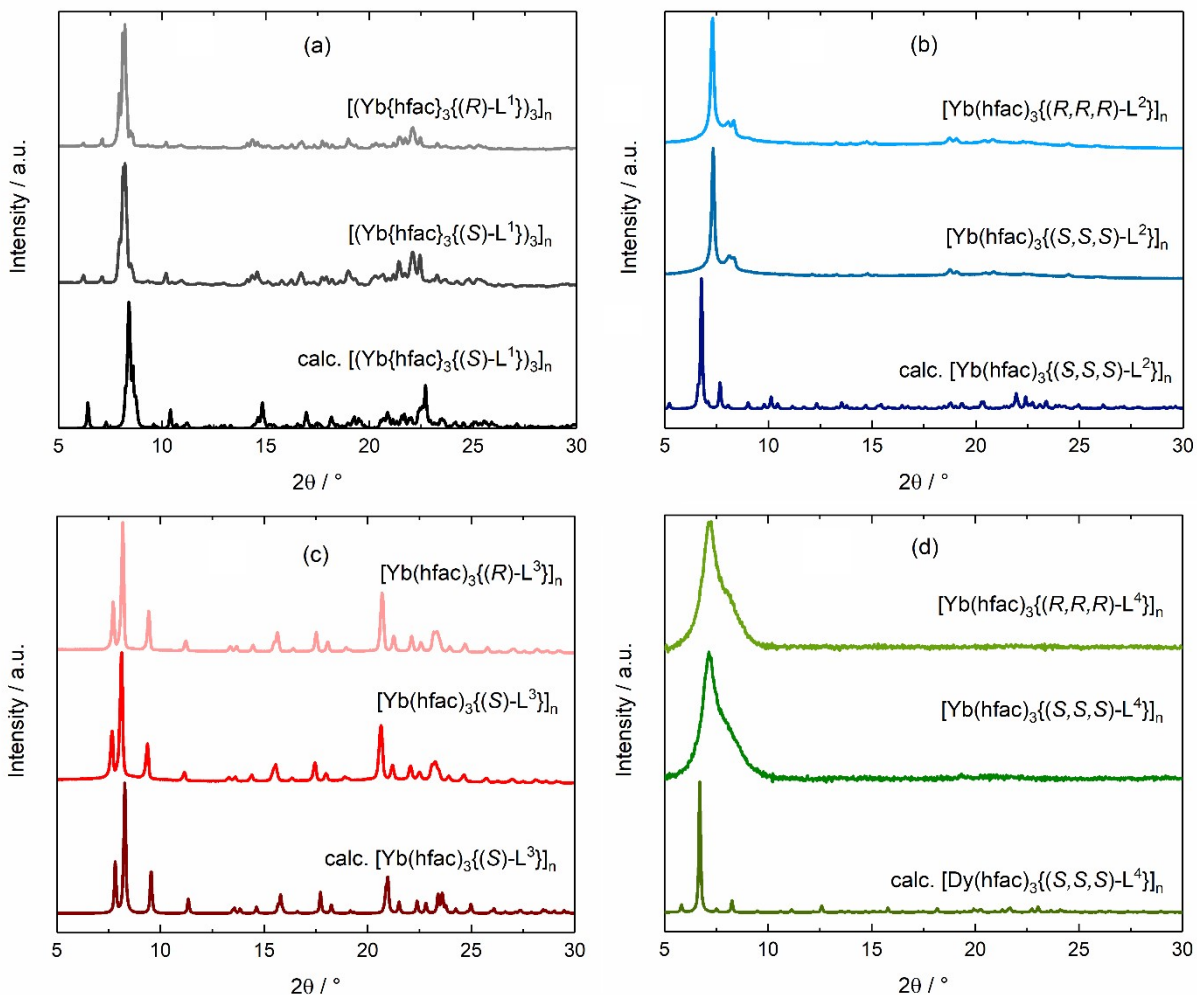


Figure S4. Superposition of experimental powder X-ray diffraction patterns measured at 300 K and simulated from single crystal data of the (*S*) enantiomer obtained at 150 K for $[(S)\text{-}1]_n$ and $[(R)\text{-}1]_n$ (a), $[(S,S,S)\text{-}2]_n$ and $[(R,R,R)\text{-}2]_n$ (b), $[(S)\text{-}3]_n$ and $[(R)\text{-}3]_n$ (c). For $[(S,S,S)\text{-}4]_n$ and $[(R,R,R)\text{-}4]_n$, the simulated data are obtained from $\{[\text{Dy(hfac)}_3((S,S,S)\text{-L}^4)]_n$ at 150 K¹.

Table S3. Energy splitting (cm^{-1}) of the ${}^2\text{F}_{7/2}$ multiplet state with wavefunction compositions and g factor values for each Kramers Doublet (KD) for $[(S)\text{-}1]_n$, $[(S,S,S)\text{-}2]_n$, $[(S)\text{-}3]_n$ and $[(S,S,S)\text{-}4]_n$.

		ΔE	g_x	g_y	g_z	Wave Function Decomposition
	$[(S)\text{-}1]_n$					
Yb1	GS	0	0.21	0.42	7.47	$90 \pm 7/2 > + 7 \pm 3/2 >$
	ES1	256	0.20	0.51	7.34	$62 \pm 5/2 > + 22 \pm 3/2 >$
	ES2	365	0.27	0.99	3.37	$48 \pm 1/2 > + 31 \pm 5/2 > + 19 \pm 3/2 >$
	ES3	466	4.83	4.10	1.21	$52 \pm 3/2 > + 42 \pm 1/2 >$
Yb2	GS	0	0.16	0.37	7.55	$91 \pm 7/2 > + 6 \pm 3/2 >$

	ES1	281	0.20	0.52	7.17	65 $ \pm 5/2\rangle + 22 \pm 3/2\rangle$
	ES2	381	0.52	1.26	3.42	51 $ \pm 1/2\rangle + 28 \pm 5/2\rangle + 18 \pm 3/2\rangle$
	ES3	481	5.26	3.49	1.19	53 $ \pm 3/2\rangle + 40 \pm 1/2\rangle$
	GS	0	0.13	0.27	7.49	90 $ \pm 7/2\rangle + 8 \pm 3/2\rangle$
Yb3	ES1	246	0.14	0.32	6.95	76 $ \pm 5/2\rangle + 18 \pm 3/2\rangle$
	ES2	383	1.51	2.02	3.40	50 $ \pm 1/2\rangle + 30 \pm 5/2\rangle + 16 \pm 3/2\rangle$
	ES3	493	0.93	2.48	6.22	47 $ \pm 3/2\rangle + 44 \pm 1/2\rangle$
[(S,S,S)-2]_n						
	GS	0	0.09	0.11	7.72	95 $ \pm 7/2\rangle$
	ES1	263	0.12	0.14	6.61	81 $ \pm 5/2\rangle + 15 \pm 3/2\rangle$
	ES2	436	0.76	1.11	3.43	48 $ \pm 3/2\rangle + 32 \pm 1/2\rangle + 16 \pm 5/2\rangle$
	ES3	548	5.46	3.61	1.10	65 $ \pm 1/2\rangle + 32 \pm 3/2\rangle$
[(S)-3]_n						
	GS	0	0.11	0.13	7.47	89 $ \pm 7/2\rangle + 7 \pm 3/2\rangle$
	ES1	280	0.31	0.43	6.47	87 $ \pm 5/2\rangle + 9 \pm 3/2\rangle$
	ES2	416	0.86	1.58	3.68	47 $ \pm 3/2\rangle + 37 \pm 1/2\rangle + 9 \pm 5/2\rangle$
	ES3	522	1.03	3.27	5.65	60 $ \pm 1/2\rangle + 37 \pm 3/2\rangle$
[(S,S,S)-4]_n						
	GS	0	0.49	0.73	7.46	91 $ \pm 7/2\rangle$
	ES1	181	0.09	0.31	7.40	61 $ \pm 5/2\rangle + 27 \pm 3/2\rangle$
	ES2	376	3.22	1.88	0.51	45 $ \pm 1/2\rangle + 31 \pm 5/2\rangle + 21 \pm 3/2\rangle$
	ES3	486	1.06	3.24	5.61	47 $ \pm 3/2\rangle + 46 \pm 1/2\rangle$

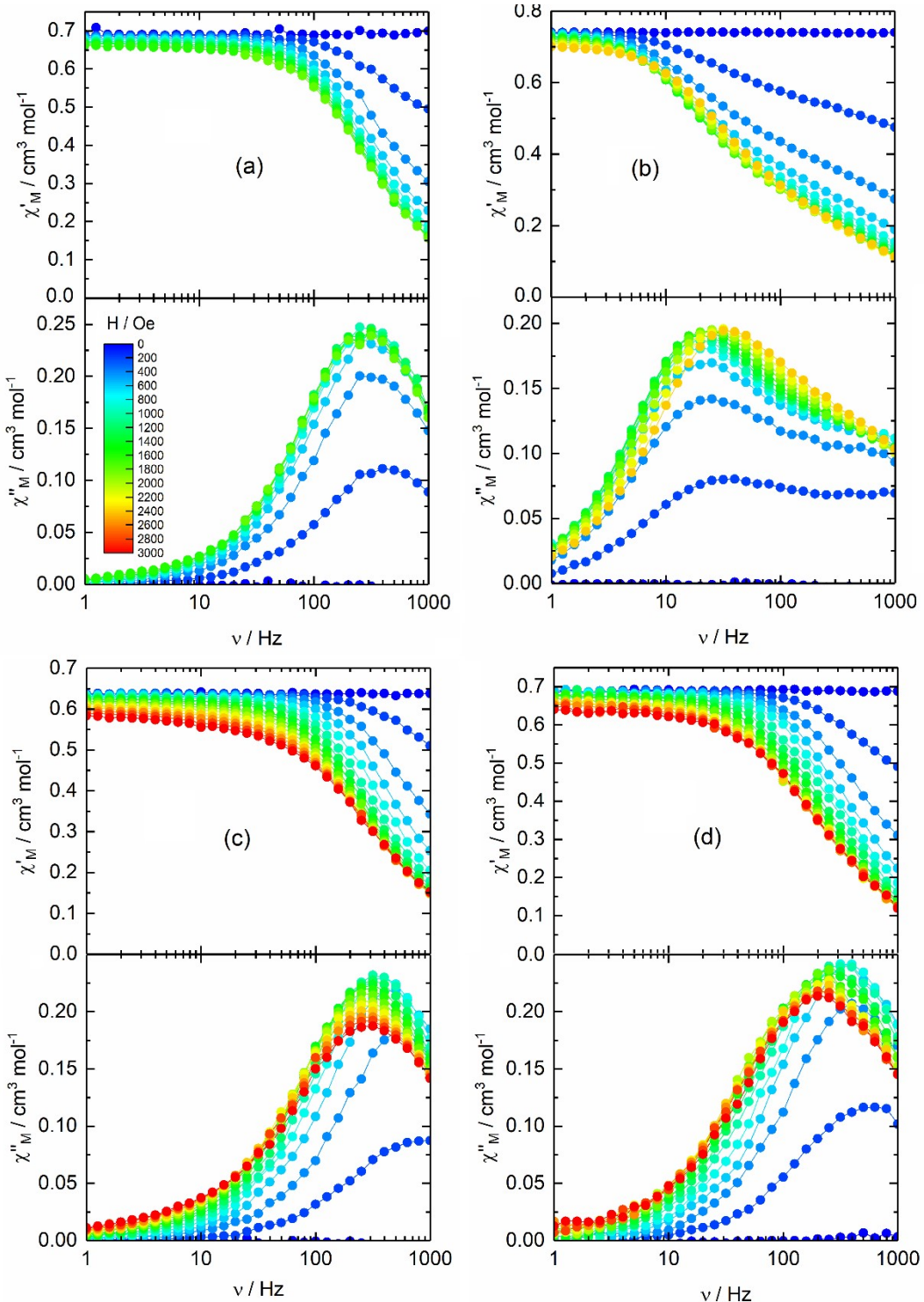


Figure S5. In-phase χ_M' and out-of-phase χ_M'' components of the ac magnetic susceptibility data for (a) $[(S)-1]_n$ from 0 to 1800 Oe at 2 K, (b) for $[(S,S,S)-2]_n$ from 0 to 2400 Oe at 2 K, (c) $[(S)-3]_n$ and (d) $[(S,S,S)-4]_n$ from 0 to 3000 Oe at 2 K.

Extended Debye model used for $[(S)-1]_n$, $[(S)-3]_n$ and $[(S,S,S)-4]_n$ (Eq. S1).

$$\chi_M' = \chi_S + (\chi_T - \chi_S) \frac{1 + (\omega\tau)^{1-\alpha} \sin\left(\alpha \frac{\pi}{2}\right)}{1 + 2(\omega\tau)^{1-\alpha} \sin\left(\alpha \frac{\pi}{2}\right) + (\omega\tau)^{2-2\alpha}}$$

$$\chi_M'' = (\chi_T - \chi_S) \frac{(\omega\tau)^{1-\alpha} \cos\left(\alpha \frac{\pi}{2}\right)}{1 + 2(\omega\tau)^{1-\alpha} \sin\left(\alpha \frac{\pi}{2}\right) + (\omega\tau)^{2-2\alpha}}$$

With χ_T the isothermal susceptibility, χ_S the adiabatic susceptibility, τ the relaxation time and α an empiric parameter which describe the distribution of the relaxation time. For SMM with only one relaxation time, α is close to zero. The extended Debye model was applied to fit simultaneously the experimental variations of χ_M' and χ_M'' with the frequency ν of the oscillating field ($\omega = 2\pi\nu$). Typically, only the temperatures for which a maximum on the χ'' vs. f curves, have been considered. The best fitted parameters τ , α , χ_T , χ_S are listed in Tables S4, S6-S7 and S9-S11 with the coefficient of determination R^2 .

Two-tau extended Debye model used for $[(S,S,S)-2]_n$ (Eq. S2).

$$\chi' = \chi_{S,tot} + (\chi_{T_1} - \chi_{S_1}) \frac{1 + (\omega\tau_1)^{1-\alpha_1} \sin\left(\frac{\pi\alpha_1}{2}\right)}{1 + 2(\omega\tau_1)^{1-\alpha_1} \sin\left(\frac{\pi\alpha_1}{2}\right) + (\omega\tau_1)^{2-2\alpha_1}} +$$

$$+ (\chi_{T_2} - \chi_{S_2}) \frac{1 + (\omega\tau_2)^{1-\alpha_2} \sin\left(\frac{\pi\alpha_2}{2}\right)}{1 + 2(\omega\tau_2)^{1-\alpha_2} \sin\left(\frac{\pi\alpha_2}{2}\right) + (\omega\tau_2)^{2-2\alpha_2}}$$

$$\chi'' = (\chi_{T_1} - \chi_{S_1}) \frac{(\omega\tau_1)^{1-\alpha_1} \cos\left(\frac{\pi\alpha_1}{2}\right)}{1 + 2(\omega\tau_1)^{1-\alpha_1} \sin\left(\frac{\pi\alpha_1}{2}\right) + (\omega\tau_1)^{2-2\alpha_1}} +$$

$$+ (\chi_{T_2} - \chi_{S_2}) \frac{(\omega\tau_2)^{1-\alpha_2} \cos\left(\frac{\pi\alpha_2}{2}\right)}{1 + 2(\omega\tau_2)^{1-\alpha_2} \sin\left(\frac{\pi\alpha_2}{2}\right) + (\omega\tau_2)^{2-2\alpha_2}}$$

With χ_T the isothermal susceptibility, χ_S the adiabatic susceptibility, τ the relaxation time and α an empiric parameter which describe the distribution of the relaxation time. For SMM with only one relaxing object α is close to zero. The extended Debye model was applied to fit simultaneously the experimental variations of χ_M' and χ_M'' with the frequency ν of the

oscillating field ($\omega = 2\pi\nu$). The best fitted parameters τ_1 , α_1 , χ_{1T} , χ_{1S} , τ_2 , α_2 , χ_{2T} and χ_{2S} are listed in Tables S5 and S12 with the coefficient of determination R^2 . τ_1 , α_1 , χ_{1T} , χ_{1S} are parameters for the high frequency contribution while τ_2 , α_2 , χ_{2T} and χ_{2S} are for the low frequency contribution.

Table S4. Best fitted parameters (χ_T , χ_S , τ and α) with the extended Debye model for compound $[(S)-1]_n$ at 2 K in the magnetic field range 200-1800 Oe.

H / Oe	χ_T / $\text{cm}^3 \text{ mol}^{-1}$	χ_S / $\text{cm}^3 \text{ mol}^{-1}$	α	τ / s	R^2
200	2.06613	1.32392	0.06390	3.69E-04	0.99996
400	2.05627	0.69620	0.07414	4.48E-04	0.9999
600	2.04831	0.42477	0.09248	4.81E-04	0.99984
800	2.03608	0.33163	0.09117	5.13E-04	0.99984
1000	2.02504	0.28789	0.09427	5.31E-04	0.9998
1200	2.01425	0.22826	0.11044	5.33E-04	0.9998
1400	2.00094	0.24108	0.10932	5.52E-04	0.99983
1600	1.98661	0.20596	0.12207	5.45E-04	0.99983
1800	1.98524	0.19571	0.13690	5.48E-04	0.99959

Table S5. Best fitted parameters ($\chi_{T,1}$, $\chi_{S,1}$, τ_1 , α_1 , ($\chi_{T,2}$, $\chi_{S,2}$, τ_2 and α_2) with the extended Debye model for compound $[(S,S,S)-2]_n$ at 2 K in the magnetic field range 200-2400 Oe.

H / Oe	$\chi_{T,1}$ / cm ³ mol ⁻¹	χ_S / cm ³ mol ⁻¹	τ_1 / s	α_1	$\chi_{T,2}$ / cm ³ mol ⁻¹	α_2	τ_2 / s	R ²
200	0.50996	0.35838	6.35E-03	0.12050	0.59300	0.38008	1.68E-04	0.99997
400	0.40147	0.14926	8.53E-03	0.08463	0.49459	0.37808	3.27E-04	0.99992
600	0.35213	0.05446	9.36E-03	0.07536	0.44961	0.38454	3.79E-04	0.99990
800	0.32361	0.00159	9.52E-03	0.07243	0.42225	0.40110	3.42E-04	0.99979
1000	0.33304	0.00181	9.88E-03	0.07098	0.41276	0.39145	4.08E-04	0.99990
1200	0.34893	0.00239	9.68E-03	0.07624	0.39332	0.37266	4.23E-04	0.99990
1400	0.34336	0.00000	9.45E-03	0.07178	0.39236	0.37306	4.55E-04	0.99989
1600	0.34147	0.00000	9.00E-03	0.07389	0.39092	0.37407	4.80E-04	0.99990
1800	0.34000	0.00000	8.43E-03	0.07293	0.38654	0.36565	4.89E-04	0.99990
2000	0.33713	0.00356	7.75E-03	0.07454	0.38777	0.36179	5.07E-04	0.99993
2200	0.34180	0.00596	6.96E-03	0.08126	0.37902	0.34912	4.93E-04	0.99995
2400	0.34556	0.00246	6.04E-03	0.09383	0.36521	0.34427	4.34E-04	0.99996

Table S6. Best fitted parameters (χ_T , χ_S , τ and α) with the extended Debye model for compound **[*(S*-3]_n** at 2 K in the magnetic field range 200-3000 Oe.

H / Oe	χ_T / cm ³ mol ⁻¹	χ_S / cm ³ mol ⁻¹	α	τ / s	R ²
200	0.63775	0.43746	0.07896	2.19E-04	0.99998
400	0.63579	0.24158	0.04842	2.95E-04	0.99994
600	0.63552	0.14293	0.06741	3.48E-04	0.99992
800	0.63348	0.10429	0.08571	4.05E-04	0.99993
1000	0.63072	0.08594	0.09915	4.58E-04	0.99992
1200	0.62818	0.07888	0.11159	5.03E-04	0.99984
1400	0.62574	0.06720	0.13670	5.27E-04	0.99985
1600	0.62117	0.06076	0.15074	5.46E-04	0.99987
1800	0.61725	0.05766	0.16217	5.59E-04	0.99989
2000	0.61183	0.05492	0.17589	5.71E-04	0.99988
2200	0.60676	0.04772	0.19199	5.69E-04	0.9999
2400	0.60121	0.04239	0.20636	5.60E-04	0.9999
2600	0.59530	0.03738	0.22038	5.48E-04	0.9999
2800	0.58899	0.03253	0.23533	5.31E-04	0.99982
3000	0.58141	0.02917	0.24432	5.15E-04	0.99975

Table S7. Best fitted parameters (χ_T , χ_S , τ and α) with the extended Debye model for compound $[(S,S,S)-4]_n$ at 2 K in the magnetic field range 200-3000 Oe.

H / Oe	χ_T / cm ³ mol ⁻¹	χ_S / cm ³ mol ⁻¹	α	τ / s	R ²
200	0.68899	0.42072	0.08032	3.16E-04	0.99991
400	0.68938	0.21577	0.08558	3.91E-04	0.99984
600	0.68893	0.11640	0.10870	4.34E-04	0.99958
800	0.68503	0.08223	0.12363	4.80E-04	0.99954
1000	0.68391	0.05567	0.15408	5.23E-04	0.99944
1200	0.68676	0.04194	0.18259	5.85E-04	0.99936
1400	0.68245	0.03885	0.19000	6.38E-04	0.99957
1600	0.68141	0.02565	0.21757	6.69E-04	0.99962
1800	0.67283	0.03096	0.20779	7.07E-04	0.99919
2000	0.66885	0.02988	0.22260	7.36E-04	0.9989
2200	0.66685	0.02320	0.22707	7.34E-04	0.9995
2400	0.66491	0.02113	0.23809	7.41E-04	0.99954
2600	0.65749	0.02816	0.23149	7.51E-04	0.99956
2800	0.65073	0.02736	0.22912	7.27E-04	0.99959
3000	0.64385	0.02979	0.22242	7.17E-04	0.99968

Table S8. Fit parameters of the different relaxation mechanisms for the τ field dependences by using Eq. 1.

Compound	B_1/s^{-1}	B_2/Oe^{-2}	$A/s^{-1}K^{-1}Oe^{-4}$	$k(T)/s^{-1}$
$[(S)-1]_n$	$1.33(9)10^3$	$1.1(2)10^{-5}$	—	$1.78(1)10^3$
$[(S,S,S)-2]_n$ (HF)	$1(1)10^4$	$6(7)10^{-5}$	—	$2.11(8)10^3$
$[(S)-3]_n$	$3.5(1)10^3$	$4.5(4)10^{-6}$	$1.0(1)10^{-12}$	$1.52(3)10^3$
$[(S,S,S)-4]_n$	$2.0(1)10^3$	$2.4(4)10^{-6}$	—	$1.23(3)10^3$
$[(S,S,S)-2]_n$ (LF)	$1.6(2)10^2$	$4(1)10^{-5}$	$4.7(1)10^{-13}$	$9.6(1)10$

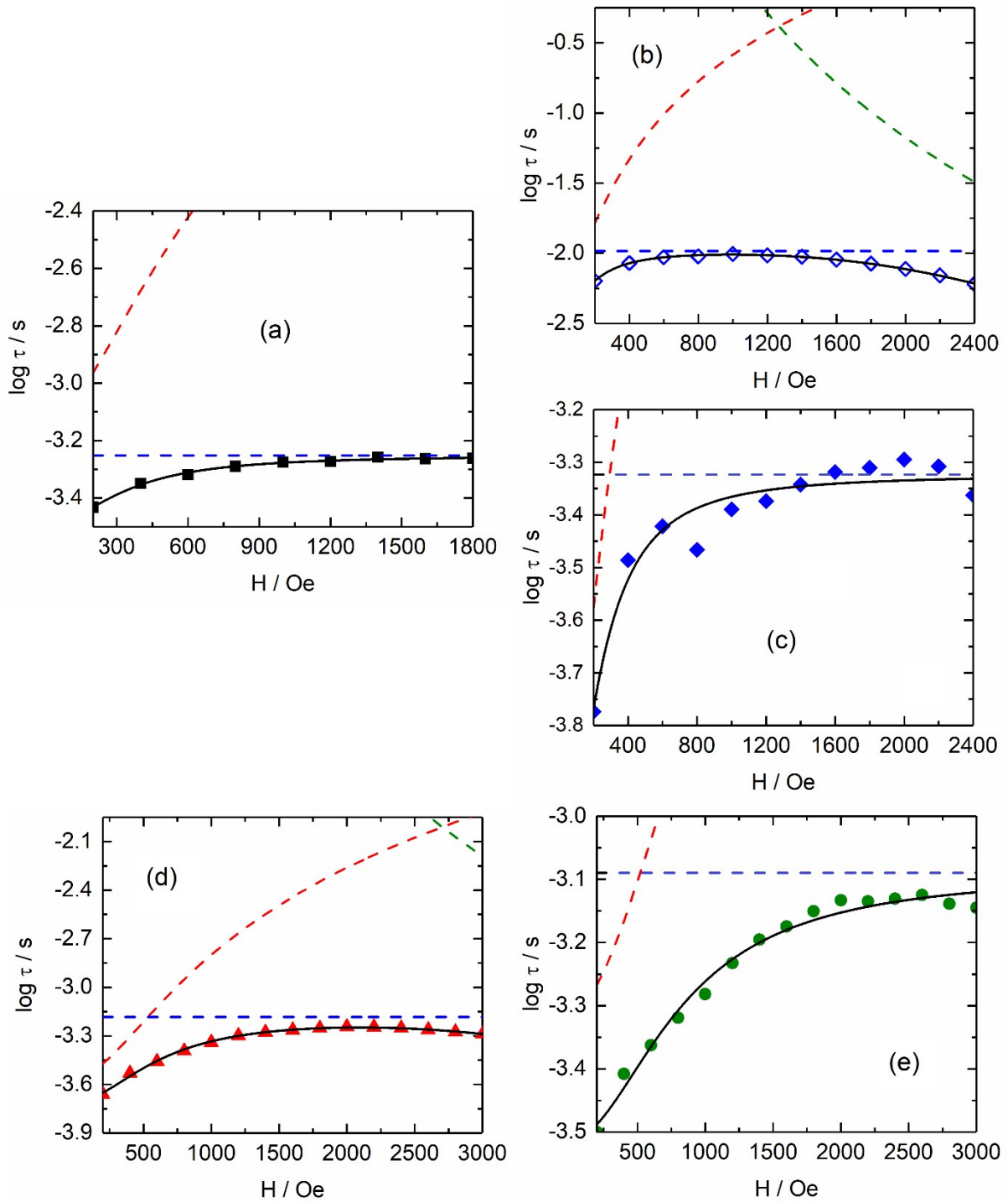


Figure S6. Field dependence of the relaxation time for $[(S)-1]_n$ from 0 to 1800 Oe at 2 K, (b) LF contribution and (c) HF contribution for $[(S,S,S)-2]_n$ from 0 to 2400 Oe at 2 K, (d) $[(S)-3]_n$ and (e) $[(S,S,S)-4]_n$ from 0 to 3000 Oe at 2 K. The black lines depict the best fits with parameters given in the table S7. Dashed red, blue and green lines are the separated QTM, field independent Orbach+Raman and direct processes, respectively.

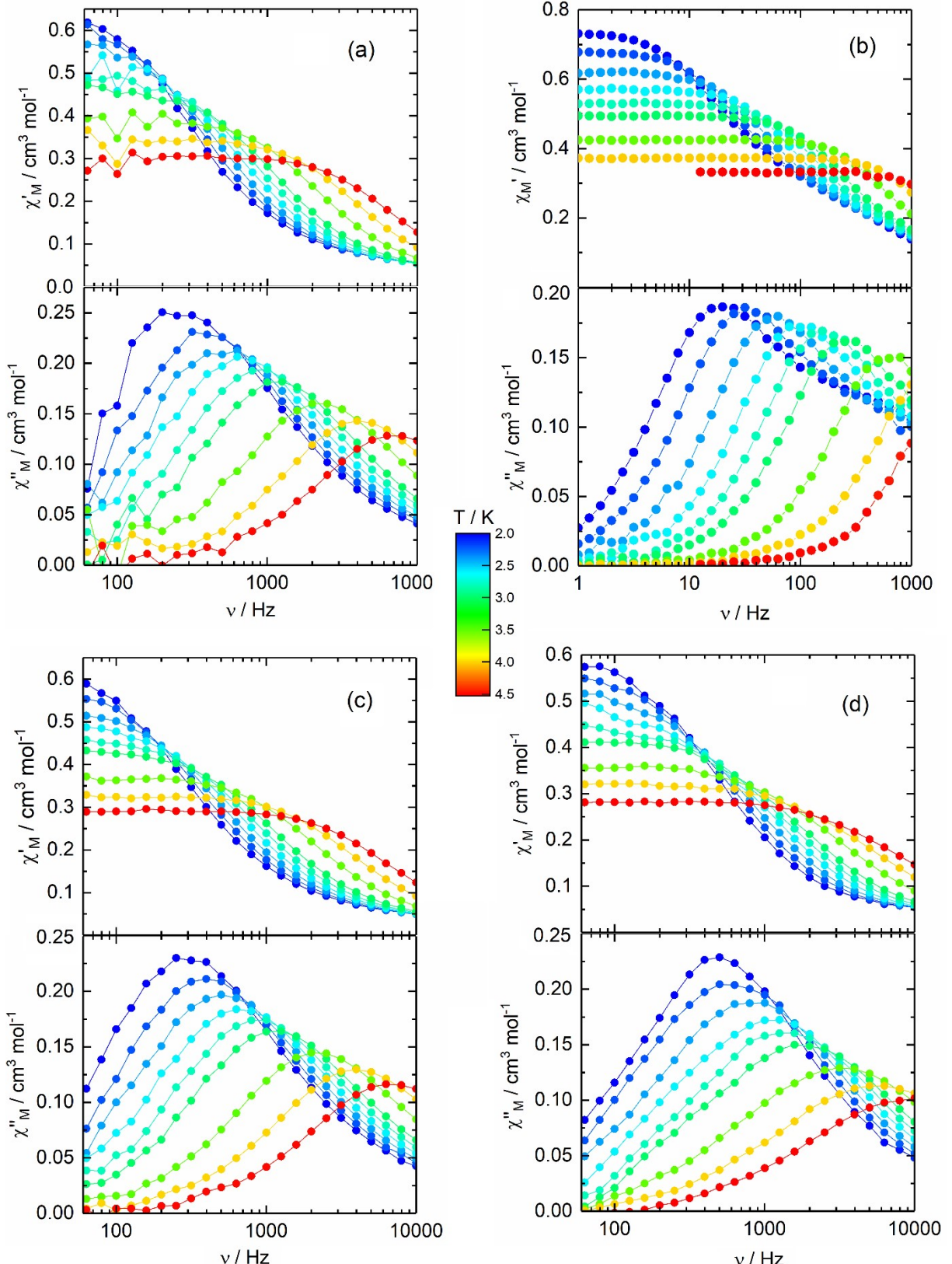


Figure S7. Frequency dependence of the in-phase χ_M' and out-of-phase χ_M'' components of the ac magnetic susceptibility data for (a) $[(S)-1]_n$, (b) $[(S,S,S)-2]_n$, (c) $[(S)-3]_n$ and (d) $[(S,S,S)-4]_n$.

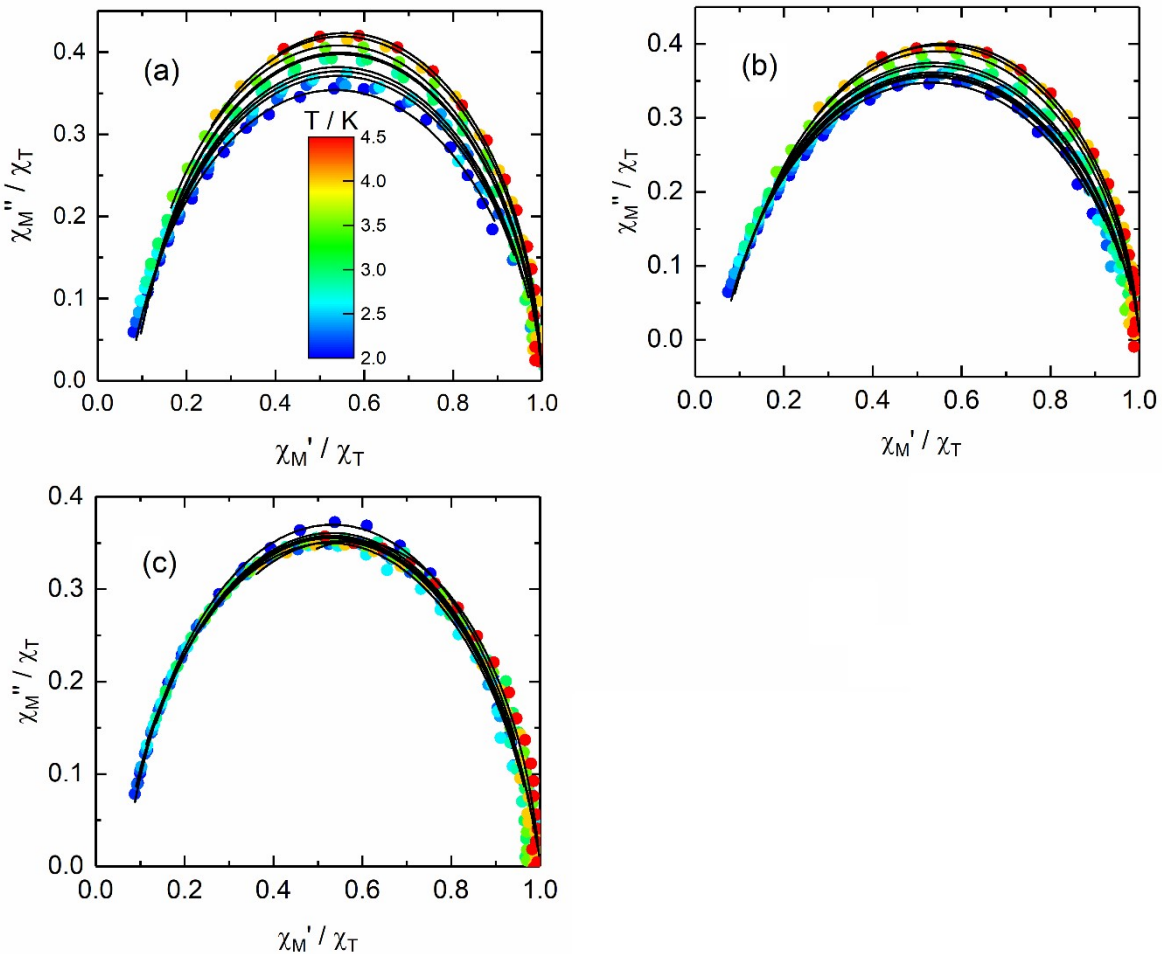


Figure S8. Normalized Cole-Cole plot for (a) $[(S)-1]_n$, (b) $[(S)-3]_n$ and (c) $[(S,S,S)-4]_n$.

Table S9. Best fitted parameters (χ_T , χ_S , τ and α) with the extended Debye model for $[(S)-1]_n$ at 1000 Oe in the temperature range 2-4.5 K.

T / K	$\chi_T / \text{cm}^3 \text{ mol}^{-1}$	$\chi_S / \text{cm}^3 \text{ mol}^{-1}$	α	τ / s	R^2
2	2.08860	0.14585	0.17178	5.02E-04	0.99924
2.2	1.88303	0.15285	0.13487	3.70E-04	0.99669
2.4	1.74499	0.14465	0.12429	2.89E-04	0.99632
2.6	1.65341	0.13978	0.11462	2.27E-04	0.99643
2.8	1.48456	0.13658	0.08457	1.66E-04	0.99641
3	1.38979	0.12721	0.08151	1.28E-04	0.99701
3.5	1.18348	0.10166	0.07165	6.77E-05	0.99964
4	1.03207	0.10328	0.04520	3.84E-05	0.99939
4.5	0.91615	0.10177	0.03104	2.33E-05	0.99955

Table S10. Best fitted parameters (χ_T , χ_S , τ and α) with the extended Debye model for compound $[(S)\text{-}3]_n$ at 1000 Oe in the temperature range 2-4.5 K.

T / K	χ_T / $\text{cm}^3 \text{ mol}^{-1}$	χ_S / $\text{cm}^3 \text{ mol}^{-1}$	α	τ / s	R^2
2	0.65826	0.04067	0.18776	5.00E-04	0.99885
2.2	0.59709	0.04022	0.17105	3.76E-04	0.99848
2.4	0.54889	0.03743	0.16536	2.89E-04	0.99899
2.6	0.50954	0.03529	0.15896	2.22E-04	0.99934
2.8	0.47020	0.03495	0.14158	1.69E-04	0.9992
3	0.44032	0.03424	0.13125	1.30E-04	0.99931
3.5	0.37340	0.03364	0.09745	6.88E-05	0.99934
4	0.32768	0.03364	0.07573	3.94E-05	0.99953
4.5	0.29284	0.03629	0.05671	2.43E-05	0.9996

Table S11. Best fitted parameters (χ_T , χ_S , τ and α) with the extended Debye model for compound $[(S,S,S)\text{-}4]_n$ at 1000 Oe in the temperature range 2-4.5 K.

T / K	χ_T / $\text{cm}^3 \text{ mol}^{-1}$	χ_S / $\text{cm}^3 \text{ mol}^{-1}$	α	τ / s	R^2
2	0.61394	0.04055	0.14728	3.09E-04	0.99969
2.2	0.58373	0.03296	0.17764	2.57E-04	0.99967
2.4	0.53601	0.02988	0.17882	1.96E-04	0.99976
2.6	0.49596	0.02477	0.19127	1.50E-04	0.99864
2.8	0.45091	0.02868	0.16389	1.13E-04	0.99892
3	0.42481	0.02620	0.17035	8.90E-05	0.99842
3.5	0.36653	0.02302	0.17340	4.94E-05	0.99915
4	0.32465	0.02694	0.16694	3.00E-05	0.99956
4.5	0.28472	0.04632	0.10941	2.08E-05	0.99918

Table S12. Best fitted parameters ($\chi_{T,1}$, $\chi_{S,1}$, τ_1 , α_1 , $\chi_{T,2}$, $\chi_{S,2}$, τ_2 and α_2) with the extended Debye model for compound [(S,S,S)-4]_n at 1000 Oe in the temperature range 2-3.5 K.

T / K	$\chi_{T,1}$ / cm ³ mol ⁻¹	χ_S / cm ³ mol ⁻¹	τ_1 / s	α_1	$\chi_{T,2}$ / cm ³ mol ⁻¹	α_2	τ_2 / s	R ²
2	0.33302	0.00181	9.88E-03	0.07097	0.41278	0.39147	4.08E-04	0.99990
2.2	0.35689	0.03632	6.01E-03	0.05280	0.36389	0.33697	3.70E-04	0.99990
2.4	0.34461	0.03565	3.34E-03	0.03792	0.31357	0.28571	2.48E-04	0.99989
2.6	0.32675	0.04410	2.03E-03	0.01455	0.28890	0.23772	2.11E-04	0.99991
2.8	0.53630	0.11129	8.13E-04	0.14453	--	--	--	0.99877
3	0.49790	0.10740	5.53E-04	0.10871	--	--	--	0.99944
3.5	0.42637	0.10831	2.56E-04	0.03009	--	--	--	0.99982

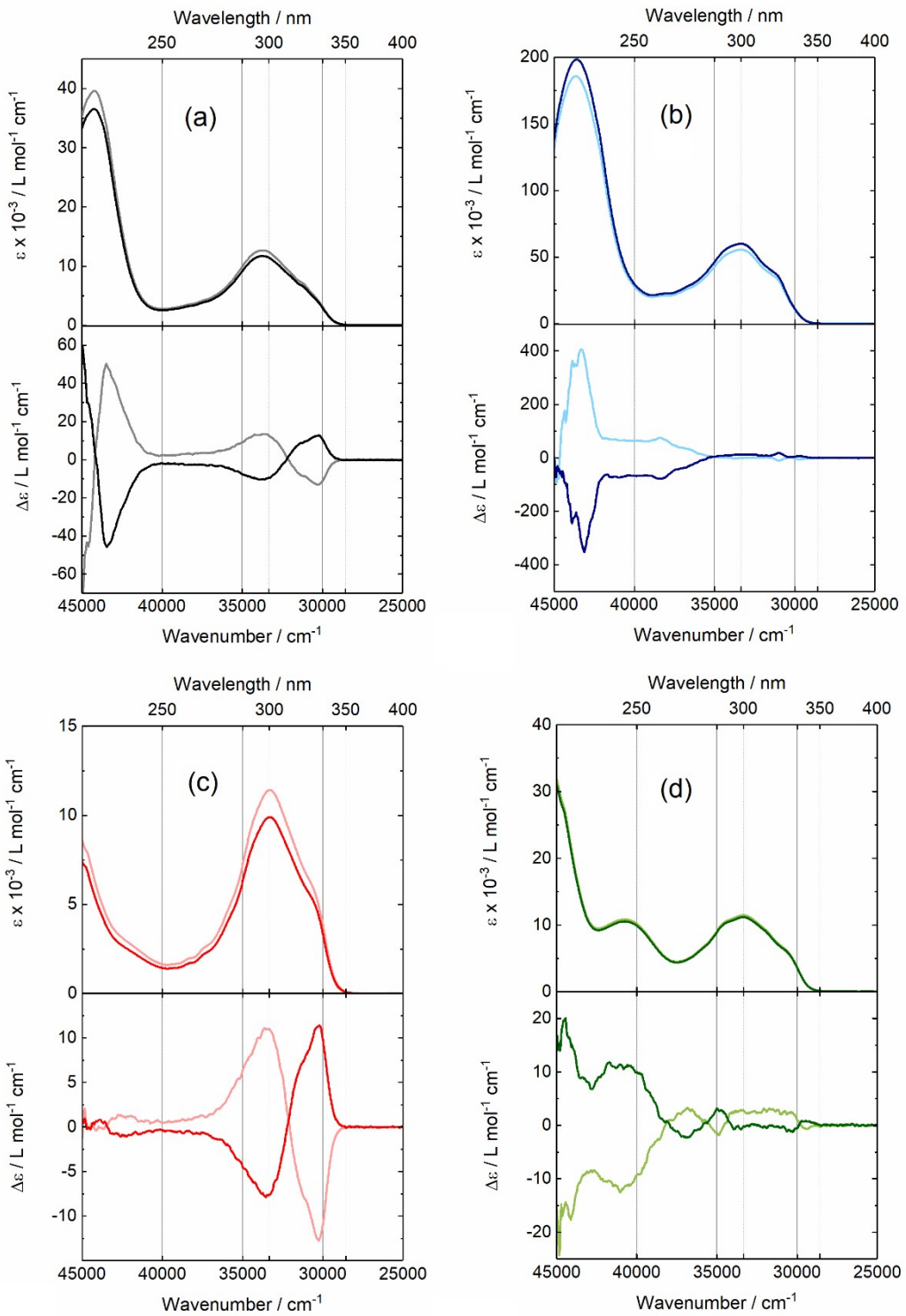


Figure S9. UV-visible absorption (top) and ECD spectra (bottom) in CH_2Cl_2 solution and room temperature for (a) $[(S)\text{-}1]$ (gray line) and $[(R)\text{-}1]$ (black line) ($C = 1 \times 10^{-5} \text{ mol L}^{-1}$), (b) $[(S,S,S)\text{-}2]$ (light blue line) and $[(R,R,R)\text{-}2]$ (dark blue line) ($C = 1 \times 10^{-5} \text{ mol L}^{-1}$), (c) $[(S)\text{-}3]$ (light red line) and $[(R)\text{-}3]$ (dark red line) ($C = 1 \times 10^{-4} \text{ mol L}^{-1}$) and (d) $[(S,S,S)\text{-}4]$ (light green line) and $[(R,R,R)\text{-}4]$ (dark green line) ($C = 5 \times 10^{-5} \text{ mol L}^{-1}$).

Table S13. Largest values of the dissymmetry factors g_{abs} for the four complexes in CH_2Cl_2 solution.

Complex	Largest $ g_{a\ b} $ factor (wavelength)
$[Y \ \mathbf{b} \mathbf{h} \ f \ \mathbf{d}_3\{(Sg/(R) - L^1)\}]$	3.50×10^{-2} ($\approx 333 \text{ nm}$)
$[Y \ \mathbf{b} \mathbf{h} \ f \ \mathbf{d}_3\{(ScS, S)/(R, R, R) - L^2\}]$	3.61×10^{-2} ($\approx 260 \text{ nm}$)
$[Y \ \mathbf{b} \mathbf{h} \ f \ \mathbf{d}_3\{(Sg/(R) - L^3)\}]$	2.92×10^{-2} ($\approx 333 \text{ nm}$)
$[Y \ \mathbf{b} \mathbf{h} \ f \ \mathbf{d}_3\{(ScS, S)/(R, R, R) - L^4\}]$	1.10×10^{-2} ($\approx 244 \text{ nm}$)

* The gabs values are calculated using the Eq. S3: $g_{\text{abs}} = \Delta\epsilon/\epsilon = (\epsilon_L - \epsilon_R)/(1/2(\epsilon_L + \epsilon_R))$ where $\Delta\epsilon = \epsilon_L - \epsilon_R$ is the difference between the left (ϵ_L) and right (ϵ_R) molar absorption coefficients at the absorption wavelength.

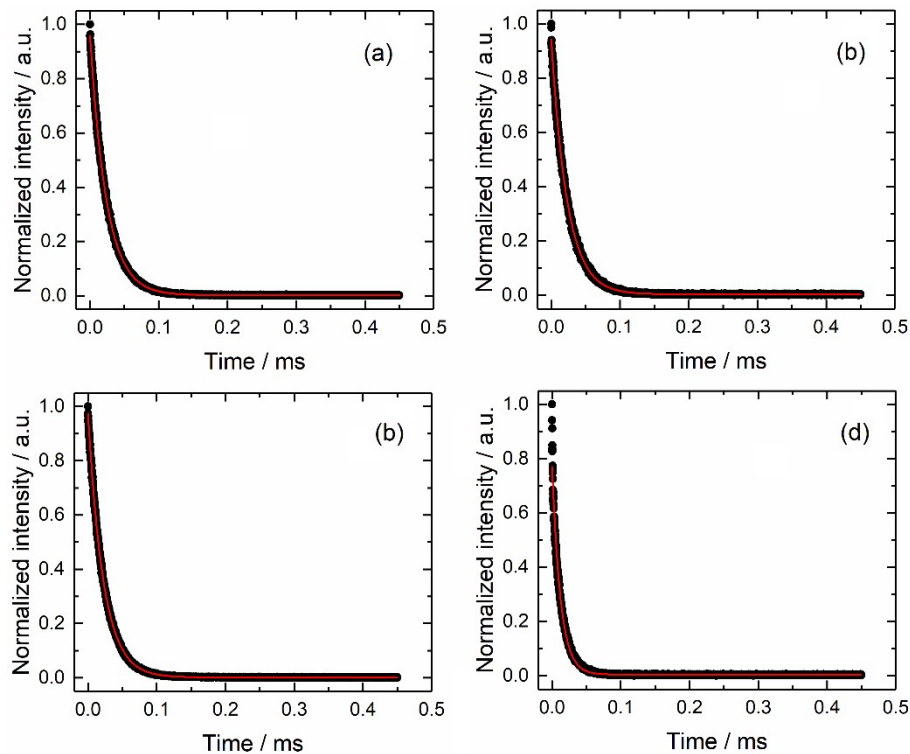


Figure S10. Emission lifetime decays (black dots) and mono-exponential fit curves (red line) for $[(S/R)-1]$ (a), $[(S,S,S/R,R,R)-2]$ (b), $[(S/R)-3]$ (c) and $[(S,S,S/R,R,R)-4]$ (d) in CH_2Cl_2 solution excited at 280 nm (35714 cm^{-1}).

Table S14. Selected dissymmetry factors g_{lum} for $[(S/R)\text{-}1]$, $[(S,S,S/R,R,R)\text{-}2]$, $[(S/R)\text{-}3]$ and $[(S,S,S/R,R,R)\text{-}4]$ in CH_2Cl_2 solution at room temperature.

[(S)-1]		[(R)-1]	
wavelength / nm	g_{lum}	wavelength / nm	g_{lum}
960	4.10E-02	960	-4.10E-02
980	-4.65E-02	980	4.50E-02
1000	/	1000	/
1030	3.82E-02	1030	-3.88E-02
[(S,S,S)-2]		[(R,R,R)-2]	
wavelength / nm	g_{lum}	wavelength / nm	g_{lum}
964	-1.8E-02	964	1.60E-02
977	5.25E-02	977	-5.21E-02
998	2.88E-02	998	-3.03E-02
1030	-2.10E-02	1030	2.25E-02
[(S)-3]		[(R)-3]	
wavelength / nm	g_{lum}	wavelength / nm	g_{lum}
960	3.85E-02	960	-4.30E-02
982	-4.58E-02	982	4.67E-02
1000	/	1000	/
1038	3.86E-02	1038	-3.90E-02
[(S,S,S)-4]		[(R,R,R)-4]	
wavelength / nm	g_{lum}	wavelength / nm	g_{lum}
957	-1.12E-02	957	8.40E-03
978	2.65E-02	978	-2.63E-02
995	1.30E-02	995	-1.25E-02
1035	-1.78E-02	1035	1.42E-02

Table S15. Selected dissymmetry factors g_{lum} for $[(S/R)\text{-}1]_n$, $[(S,S,S/R,R,R)\text{-}2]_n$, $[(S/R)\text{-}3]_n$ and $[(S,S,S/R,R,R)\text{-}4]_n$ in solid-state at room temperature.

$[(S)\text{-}1]_n$		$[(R)\text{-}1]_n$	
wavelength / nm	g_{lum}	wavelength / nm	g_{lum}
986	2.38E-03	986	-2.33E-03
1019	-1.82E-03	1019	4.49E-03
$[(S,S,S)\text{-}2]_n$		$[(R,R,R)\text{-}2]_n$	
wavelength / nm	g_{lum}	wavelength / nm	g_{lum}
976	-1.15E-02	976	1.13E-02
998	1.52E-02	998	-6.04E-03
1025	-1.59E-02	1025	1.72E-02
$[(S)\text{-}3]_n$		$[(R)\text{-}3]_n$	
wavelength / nm	g_{lum}	wavelength / nm	g_{lum}
973	7.95E-03	973	-6.65E-03
990	-8.52E-03	990	1.24E-02
1020	1.16E-02	1020	-1.31E-02
$[(S,S,S)\text{-}4]_n$		$[(R,R,R)\text{-}4]_n$	
wavelength / nm	g_{lum}	wavelength / nm	g_{lum}
974	-8.40E-03	974	9.04E-03
986	9.23E-03	986	-9.48E-03
1025	-1.18E-02	1025	1.42E-02

Reference

- 1 C. A. Mattei, V. Montigaud, V. Dorcet, F. Riobé, G. Argouarch, O. Maury, B. Le Guennic, O. Cador, C. Lalli and F. Pointillart, *Inorg. Chem. Front.* 2021, **8**, 963